Synthesis of Fluorophore-Tagged Xylosides That Prime Glycosaminoglycan Chains

Vy M. Tran[†,‡] and Balagurunathan Kuberan*[,†,‡]

‡Departments of Medicinal Chemistry and †Bioengineering, University of Utah, Salt Lake City, Utah 84112, United States

S *Supporting Information*

ABSTRACT: Biosynthesis and functions of glycosaminoglycan (GAG) chains are complex and remain elusive. To better understand the factors that regulate the biosynthesis and functions, fluorophore-tagged xylosides carrying two different linkages between fluorophore and xylose residue were synthesized and evaluated for their ability to prime GAG chains such as heparan sulfate (HS), chondroitin sulfate (CS), and dermatan sulfate (DS) in various cell lines. These in vitro studies resulted in the identification of fluorophore-tagged xylosides that prime high molecular weight GAG chains. Primed GAG chains carrying a fluorophore group has several advantages for studying the factors that regulate the biosynthesis, analyzing intact fine structures at low detection limits, and setting the stage for studying structure−function relations of GAG chains of cellular origin.
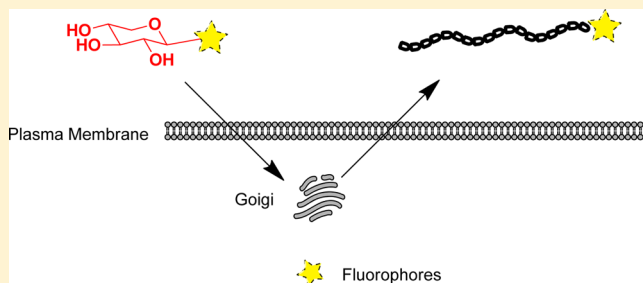
INTRODUCTION

Proteoglycans modulate numerous pathophysiological functions such as development, angiogenesis, axonal growth, anticoagulation, cancer progression, microbial pathogenesis, and so forth.[1−4] The quantity and quality of GAG structures, made by various cells, are dynamically regulated in a spatiotemporal manner during the development of an organism and during the normal aging of an organism, as well as during the progression of several pathological conditions.[5,6] Profiling and deciphering dynamic changes in GAG structures will provide new avenues to diagnose disease states and may thwart those conditions with novel therapeutics.[7] Most of these structural changes have been deduced using radiolabeled monosaccharides and sulfate as biosynthetic precursors in various cellular systems. However, these radiolabeled precursors cannot be used in organisms as they pose toxicity and other challenges. Several β-xyloside derivatives have been shown to act as acceptors and substitute for core proteins in vivo as well as in vitro in the production of core protein free GAG chains.[8−14] Fluorophore-tagged xylosides that are able to prime GAG chains will be an excellent tool to study the structure−function relationship in vivo. Commercial 4-methyl-umbelliferyl-β-D-xyloside (UMB-*O*-xyloside) has been shown until now to function as acceptor for the elongation of GAG chains; however, UMB-*O*-xylosides prime mostly CS chains or small oligossacharides.[15−17] Earlier studies examined several other fluorophore-tagged xylosides for studying the mechanism of GAG biosynthesis and GAG priming activity.[18] These studies have shown successful internalization of fluorophore-conjugated xylosides into the para- and perinuclear regions of the cells. However, these molecules were unfortunately not found to initiate GAG biosynthesis suggesting that either these fluorophore xylosides failed to reach GAGOSOMES where GAG biosynthetic enzymes reside within the complex Golgi apparatus or biosynthetic enzymes could not recognize these fluorophore-conjugated xylosides after these molecules reach GAGOSOMES. It has been known that both the structure of the (fluorophore) aglycone and the type of linkage between the (fluorophore) aglycone and xyloside can affect the priming activity of xylosides.[9,10,18] Our efforts are, therefore, focused on the synthesis of expanded repertoire of fluorophore-tagged xylosides, based on developments in our lab and other laboratories, and screening of these novel xylosides for their ability to prime GAG chains in a given cellular system and provides novel avenues to profile and elucidate cellular GAG signatures in a robust manner, and assist in establishing cell-specific GAG−protein interactions.

EXPERIMENTAL SECTION

General Synthetic Procedures. All chemical reactions were carried out under a nitrogen atmosphere in oven-dried glassware using standard techniques. ^{1}H and ^{13}C NMR spectra were obtained on a Bruker 400-MHz spectrometer. Chemical shifts are relative to the deuterated solvent peak or the tetramethylsilane (TMS) peak at (δ 0.00) and are in parts per million (ppm). High-resolution mass spectrometry (HRMS) was performed using a Finnigan LCQ mass spectrometer in either positive or negative ion mode. Thin layer chromatography (TLC) was done on 0.25-mm-thick precoated silica gel aluminum sheets. Chromatograms were observed under short

and long wavelength UV light, and were visualized by heating plates that were dipped in a solution of Von's reagent containing ammonium (VI) molybdate tetrahydrate (12.5 g) and cerium (IV) sulfate tetrahydrate (5.0 g) in 10% aqueous sulphuric acid (500 mL). Flash column chromatography was performed using silica gel 60 (230−400 mesh) and employed a stepwise solvent polarity gradient, correlated with TLC mobility, and were run under pressure of 5−7 psi. HPLC was used to purify final products using C18 column (VYDAC 2.2 cm × 25 cm) with solvent A (25 mM formic acid) and solvent B (95% acetonitrile) at a flow rate of 5 mL/min in a linear gradient over 120 min starting with 0% B.

N-(β-D-xylopyranosyl) Azide (5). 2,3,4-Tri-*O*-acetyl-β-D-xylopyranosyl azide **S1** (0.1 mmol) was taken in dry methanol and was treated with freshly prepared 0.5 M solution of CH_3ONa (0.1 mL) in dry methanol at room temperature for 3 h. Neutralization with H^+ resin followed by concentration at reduced pressure gave a syrupy liquid, which was purified by silica flash column chromatography to give the title compound **5**.

Propargyl UMB Derivative (11). To the solution (10 mL) of UMB derivative (**10a** and **10b**) (1 mmol) in acetone was added potassium carbonate (3 mmol). The reaction mixture was stirred for 30 min at room temperature. Propargyl bromide (3 mmol) was then added and the mixture was stirred overnight. The reaction mixture was concentrated. The resulting crude material was dissolved in ethyl acetate, washed with water and saturated sodium chloride solution, dried over Na_2SO_4, and rotary evaporated under reduced pressure. The residue was purified by column chromatography to give the compound **11**.

Synthesis of Fluorophore-Tagged Xylosides with Amide Linkages (2, 3, 4, 7, 8, and 9). N-(β-D-xylopyranosyl) aminoacetamide **1** or N-(β-D-xylopyranosyl) amine **6** (0.1 mmol) was dissolved in dry DMF (10 mL). Di-isopropylethylamine (0.1 mmol) was added. The whole mixture was stirred for 30 min before adding the commercially available activated fluorescent reagents (Dansyl chloride, FITC and N-hydroxysuccinimidyl-1-pyrene butyrate) (1 mmol). The reaction mixture was stirred for 4 h and purified by C18-HPLC column.

Synthesis of Fluorophore-Tagged Xylosides with Click Linkages (13a and 13b). To a solution of alkyne (1 mmol) and azide (1 mmol) in DMF and water (4:1.3) solvent mixture were added sodium ascobate (0.8 mmol) followed by $Cu_2SO_4 \cdot 5H_2O$ (0.4 mmol) at room temperature, and the mixture was stirred for 12 h or until disappearance of one of the starting materials as indicated by TLC. At the end of the reaction as confirmed by TLC analysis, the solvent of the reaction mixture was evaporated using rotary-evaporator under reduced pressure. The reaction mixture was purified by flash chromatography columns as described above. The purified acetylated product (0.1 mmol) was taken in dry methanol and was treated with freshly prepared 0.5 M solution of CH_3ONa (0.1 mL) in dry methanol at room temperature for 3 h. Neutralization with H^+ resin followed by concentration at reduced pressure gave a syrupy liquid, which was purified on HPLC using C18 column to give the desired deprotected xyloside derivatives. All xylosides were characterized using Bruker 400 MHz NMR spectrometer, and structural data are furnished below:

Compound 2. ^{1}H NMR (CD_3OD): δ 8.57 (d, J = 8.6 Hz, 1H), 8.34 (d, J = 9.0 Hz, 1H), 8.20 (d, J = 7.45 Hz, 1H), 7.60 (t, J = 8.0 Hz, 1H), 7.57 (t, J = 8.0 Hz, 1H), 7.28 (d, J = 7.8 Hz, 1H), 4.70 (d, J = 9.0 Hz, 1H), 3.75 (dd, J = 5.1, 11.3 Hz, 1H),

3.56 (d, J = 3.9 Hz, 2H), 3.44−3.37 (m, 1H), 3.20−3.05 (m, 3H), 3.89 (s, 6H). Mass (ESI): calcd for $C_{19}H_{24}N_3O_7S$ [M-H]$^-$ 438.475, found 438.310.

Compound 3. ^{1}H NMR (CD_3OD): δ 8.52 (s, 1H), 8.18 (d, J = 2.0 Hz, 1H), 7.81 (dd, J = 2.0, 8.2 Hz, 1H), 7.16 (d, J = 8.2 Hz, 1H), 6.83 (d, J = 8.6 Hz, 2H), 6.67 (d, J = 2.4 Hz, 1H), 6.57 (dd, J = 2.3, 8.6 Hz, 2H), 4.38 (d, J = 11.3 Hz, 1H), 3.85 (d, J = 5.1, 11.3 Hz, 1H), 3.50−3.46 (m, 1H), 3.39−3.24 (m, 3H), 3.89 (s, 6H). Mass (ESI): calcd for $C_{28}H_{26}N_3O_{10}S$ [M+H]$^+$ 596.134, found 596.139.

Compound 4. ^{1}H NMR (CD_3OD): δ 8.37 (d, J = 9.4 Hz, 1H), 8.19−8.13 (m, 4H), 8.04−7.97 (m, 3H), 7.92 (d, J = 7.8 Hz, 1H), 3.91 (dd, m, 2H), 3.80 (dd, J = 5.1, 11.1 Hz, 1H), 3.48−3.21 (m, 7H), 2.44 (t, J = 7.4 Hz, 2H), 2.21−2.16 (m, 2H). Mass (ESI): calcd for $C_{27}H_{28}N_2O_6Na$ [M+Na]$^+$ 499.185, found 499.067.

Compound 7. ^{1}H NMR (CD_3OD): δ 8.55 (d, J = 8.6 Hz, 1H), 8.32 (d, J = 8.6 Hz, 1H), 8.20 (d, J = 7.4 Hz, 1H), 7.64 (s, 1H), 7.58 (dd, J = 7.8, 10.2 Hz, 1H), 7.56 (dd, J = 7.4, 8.6 Hz, 1H), 7.27 (d, J = 7.42 Hz, 1H), 5.34 (d, J = 9.0 Hz, 1H), 4.17 (s, 2H), 3.96 (dd, J = 5.5, 11.4 Hz, 1H), 3.68 (t, J = 9.0 Hz, 1H), 3.66−3.58 (m, 1H), 3.45−3.38 (m, 2H), 3.89 (s, 6H). Mass (ESI): calcd for $C_{20}H_{25}N_5O_6SNa$ [M+Na]$^+$ 486.142, found 486.200.

Compound 8. ^{1}H NMR (CD_3OD): δ 8.16 (2H, d, J = 16.4 Hz), 7.74 (1H, d, J = 8.2 Hz), 7.15 (1H, d, J = 8.2 Hz), 6.66 (3H, d, J = 2.0 Hz), 6.53 (2H, d, J = 8.6 Hz), 5.50 (1H, d, J = 9.4 Hz), 4.96 (2H, s), 3.90 (1H, dd, J = 5.0, 11.1 Hz), 3.88 (1H, t, J = 8.6 Hz), 3.70−3.63 (1H, m), 3.50−3.42 (2H, m). Mass (ESI): calcd for $C_{29}H_{24}N_5O_9SNa$ [M-H+Na]$^+$ 641.137, found 641.333.

Compound 9. ^{1}H NMR (CD_3OD): δ 8.27−7.84 (m, 10H), 5.46 (d, J = 9.4 Hz, 1H), 4.45 (d, J = 2.3 Hz, 1H), 3.95 (dd, J = 5.5, 11.3 Hz, 1H), 3.86 (t, J = 8.4 Hz, 1H), 3.67−3.57 (m, 3H), 3.49−3.39 (m, 2H), 2.35 (round, 2H), 2.12 (round, 2H). Mass (ESI): calcd for $C_{28}H_{28}N_4O_5Na$ [M+Na]$^+$ 523.196, found 523.130.

Compound 13a. ^{1}H NMR (CD_3OD): δ 8.30 (s, 1H), 7.70 (d, J = 9.6 Hz, 1H), 7.05 (s, 1H), 7.03 (s, 1H), 6.17 (s, 1H), 5.53 (d, J = 9.0 Hz, 1H), 5.29 (2H, s), 4.00 (dd, J = 5.5, 11.3 Hz, 1H), 3.90 (t, J = 9.0 Hz, 1H), 3.70−3.64 (m, 1H), 3.52−3.44 (m, 2H), 2.44 (s, 3H). Mass (ESI): calcd for $C_{18}H_{19}N_3O_7Na$ [M+Na]$^+$ 412.122, found 412.200.

Compound 13b. ^{1}H NMR (CD_3OD): δ 8.32 (s, 1H), 7.69 (d, J = 9.0 Hz, 1H), 7.17 (d, J = 2.3 Hz, 1H), 7.10 (dd, J = 2.3, 9.0 Hz, 1H), 6.71 (s, 1H), 5.54 (d, J = 9.0 Hz, 1H), 5.33 (2H, s), 4.00 (dd, J = 5.5, 11.3 Hz, 1H), 3.90 (t, J = 9.0 Hz, 1H), 3.71−3.64 (m, 1H), 3.52−3.44 (m, 2H). Mass (ESI): calcd for $C_{18}H_{16}F_3N_3O_7Na$ [M+Na]$^+$ 466.094, found 466.098.

Screening of Fluorophore-Tagged Xylosides in Cell Culture. The priming of the xylosides in xylosyl transferase-deficient CHO cell line *pgsA*-745 was performed as described in our earlier communication. Briefly, 1×10^5 cells were plated per well, containing the appropriate complete growth medium, in a 24-well plate and incubated at 37 °C in a humidified incubator for 24 h to reach a confluency of about 50%. The cells were then washed with sterile PBS and replaced with 450 μL appropriate medium containing 10% dialyzed FBS. A serial dilution of the primers at 100× the final concentration was prepared and 5 μL of appropriate 100× primer was added to various wells to yield final concentrations respectively. 50 μCi 6-^{3}H-glucosamine was then added to each well for radiolabeling the GAG chains synthesized. The 24-well plates were placed in

Scheme 1. Synthesis of Fluorophore-Tagged Xylosides with Amide Linkages
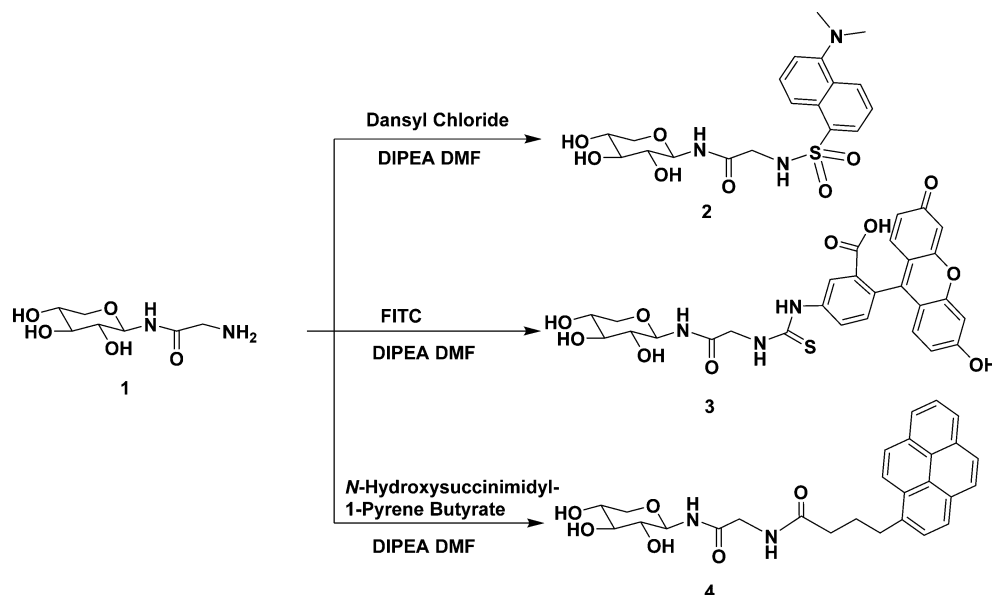
Scheme 2. Synthesis of Fluorophore-Tagged Xylosides with Triazoyl Linkages
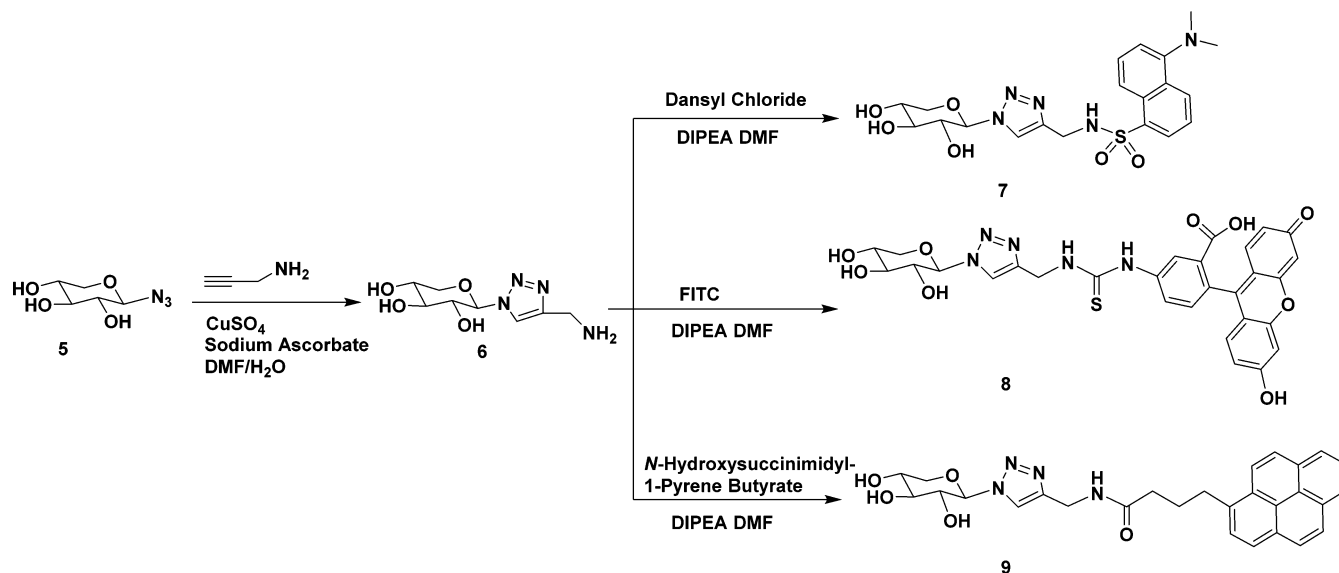
the incubator for 24 h before the addition of 6× Pronase solution (100 μL) followed by incubation at 37 °C overnight.

Purification and Quantification of GAGs. The entire contents of the wells were transferred to a microcentrifuge tube and subjected to centrifugation at 16 000×*g* for 5 min. The supernatant was transferred to a fresh tube and half-a-volume of 0.016% Triton X-100 was added. The diluted supernatant was loaded on to a DEAE-sepharose column (0.2 mL) pre-equilibrated with 10 column volumes of wash buffer (20 mM NaOAc buffer (pH 6.0) containing 0.1 M NaCl and 0.01% Triton X-100) and the column was washed with 20 column volumes of wash buffer. The bound HS/CS was eluted using 6 column volumes elution buffer (20 mM NaOAc (pH 6.0) containing 1 M NaCl). The amount of GAG primed by various xylosides was determined by quantifying the ^{3}H-radioactivity incorporated in the purified HS/CS eluate. 50 μL of the various eluates was diluted with 5 mL of scintillation cocktail and

triplicate samples were measured using a scintillation counter for total radioactivity.

Analysis of Primed GAG Chains. The chain length of the primed GAG was determined by measuring the migration time on two tandem G2000SWXL (Tosoh, 7.8 mm × 30 cm) size exclusion columns using the HPLC Hitachi system with an inline radiodetector or fluorescent detector. The solvent containing phosphate (100 mM KH$_2$PO$_4$, 100 mM NaCl, pH 6) was used as an eluent. The average molecular weight was determined by measuring the migration time of GAG chains in comparison to those of polystyrene sulfonate standards examined under similar conditions.

The HS/CS composition of the primed GAG chains was determined by digesting the GAG chains with heparitinase I/II/III or chondroitinase ABC enzymes. The solution containing GAGs was diluted to 0.2 M NaCl, followed by the addition of heparitinase or chondroitinase ABC buffer and 5 mU of heparitinase I/II/III or chondroitinase ABC enzyme. The

Scheme 3. Synthesis of Umbelliferyl Xylosides with Triazoyl Linkages
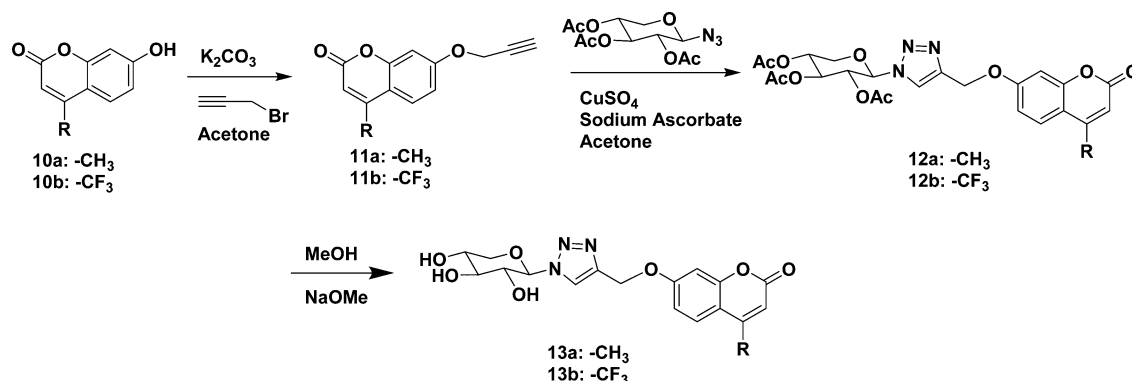
reaction mixture was incubated at 37 °C for 2 h, the solution was then loaded on to two tandem G2000 SWXL columns (7.8 mm × 30 cm) and analyzed with the aid of an inline radiometric detector using phosphate buffer (100 mM KH$_2$PO$_4$, 100 mM NaCl, pH 6) as an eluent. The percentage of HS/CS was determined based on the percentage area of undigested and digested GAG peaks.

RESULTS AND DISCUSSION

Several fluorophore-tagged xylosides were synthesized and examined to determine whether these fluorophore-tagged xylosides can elongate GAG chains. These fluorophore-tagged xylosides offer prospects to further our understanding of factors that regulate GAG biosynthesis as well as new knowledge on the role of GAG chains in various signaling events associated with pathophysiological processes.

Synthesis of Fluorophore-Tagged Xylosides. Several studies proved that stimulation of GAG chains is affected not only by hydrophobic aglycones of xylosides, but also by their glycosidic linkages.[8,12−14,19] Therefore, several fluorophore-tagged xylosides with amide and triazole in the glycosidic linkage were synthesized in this study. N-(2,3,4-Trihydroxyl-β-xylopyranosyl) acetamide **1** was synthesized from xylosyl azide as outlined in Supporting Information (Scheme S1).[20] Fluorophore-tagged xylosides (**2**, **3**, and **4**) were synthesized from corresponding commercially available activated fluorescent reagents (dansyl chloride, FITC, and N-hydroxysuccinimidyl-1-pyrene butyrate) by reacting with the xyloside **1** that contains the reactive amine group (Scheme 1).

It is known that the linker between xylose and the aglycone moiety (fluorophore-tag in this case) may dramatically influence the priming activity. Therefore, a second strategy was devised in which xylose was differentially attached to fluorescent tags by reacting xylosyl azide **5** with triple bond containing amine groups using click chemistry as shown in Scheme 2.[21] Xyloside **6** with a triazoyl linkage is prepared, which contains the reactive amine group for conjugating with activated fluorescent reagents to obtain the fluorophore-tagged xylosides with triazoyl linkages (**7**, **8**, and **9**).

The commercial, well-known UMB-O-xyloside primes mostly short chains of GAG chains or oligosaccharides in various cell types.[15,17] Click chemistry was used to conjugate fluorescent UMB derivatives **10a** and **10b** to the xylose unit. Fully acetylated xyloside was reacted with UMB derivatives containing a triple bond and these UMB-click-xylosides were deprotected under Zemplen condition to obtain the final products **13a** and **13b**, as outlined in Scheme 3. All final

products were purified on a reverse phase C18 column using HPLC as described in the Experimental Section, followed by structural analysis using NMR and MS.

Screening of Fluorophore-Tagged Xylosides. The priming activity of these novel xylosides may perhaps be attributed to the presence of a very hydrophobic fluorescent group, helping their transport across the cell surface and Golgi membranes. At the beginning, the priming ability of fluorophore-tagged xylosides are investigated using a mutant Chinese hamster ovary (CHO) cell line, pgsA-745, which lacks active xylosyltransferase enzyme.[22] This cell line does not make HS, CS, or DS chains, as the assembly of these GAG chain types requires the xylosylation of core proteins by xylosyltransferase. It requires the exogenous supply of β-xylosides to produce GAG chains such as HS, CS, and DS, and is thus a convenient cellular system to ascertain the quantity of the primed GAG chains by exogenously supplied fluorophore-tagged xylosides. Neither dansyl group attached xylosides (**2** and **7**) nor fluorescein attached xylosides (**3** and **8**) primed any detectable GAG chains. It may perhaps be due to the presence of charged amine (in dansyl moiety) and carboxyl (in fluorscein moiety) groups preventing the uptake of xylosides across the cell membrane. This is in accordance with Johnsson et al. who found out that the dansyl group attached xylosides were unable to prime any detectable amount of GAG chains.[18] Fluorophore-tagged xylosides without a charged group are next chosen to be synthesized. Fluorophore-tagged xylosides (**4**, **9**, **13a**, and **13b**), in which xylose residue is attached to 1-pyrene butyrate and UMB derivatives, were synthesized. Pyrene containing xyloside with amide linkages **4** was not able to prime GAG chains, while the pyrene containing xyloside with triazoyl linkage **9** was able to prime at various concentrations. It is interesting to observe that the pyrene containing xyloside with triazoyl linkage **9** can prime GAG chains, but the pyrene containing xyloside with amide linkage **4** cannot prime GAG chains. It is predicted that the triazoyl ring may increase the diffusion rate and direct the primer to Golgi compartments.

Next, UMB-click-xylosides **13a** and **13b** were compared to the commercial UMB-O-xylosides that prime mostly GAG chains with a short chain length. The priming activities of the UMB-click-xylosides **13a** and **13b** and the commercial xyloside were compared at various concentration (50 μM, 100 μM, 300 μM, 600 μM, and 1 mM) (Figure 1). It is interesting to note that priming activity of the UMB-click-xylosides **13a** and **13b** was concentration-dependent but the UMB-O-xyloside was not. We also tested the priming activity of UMB-click-xylsoides **13a** and **13b** in endothelial cells (BLMVEC). Both UMB-click-
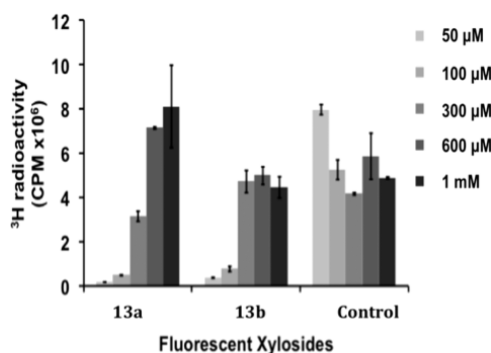
Figure 1. Priming activity of UMB-click-xylosides (**13a**, **13b**) and UMB-*O*-xylosides (control) in *pgsA*-745 cell line. CHO cells were treated with fluorophore-tagged xylosides at 50 μM, 100 μM, 300 μM, 600 μM, and 1 mM in the presence of ^{3}H(100 μCi) as described in the Experimental Section. The GAG chains were purified by anion exchange chromatography and quantitated using a liquid scintillation counter. The results were the average of two independent experiments.

xylosides primed GAG chains very well in BLMVEC cells at various concentrations.

Structural Analysis of Primed GAG Chains in CHO Cells. The GAG chains primed by these fluorophore-tagged xylosides **9**, **13a**, and **13b** were further analyzed for their molecular weights using size exclusion columns, as outlined in the Experimental Section. The chain length of GAG chains primed by fluorophore-tagged xyloside **9** in CHO cells was determined by measuring the migration time of GAG chains in comparison to those of polystyrene sulfonate standards performed under similar conditions on the size exclusion column and suggests that GAG chains, primed by fluorophore-tagged xyloside **9** in CHO cells, have 27 KDa at 50 μM and 20 KDa at 100 μM (Figure S1). However, the fluorophore-tagged xyloside **9** was not sensitive enough; therefore, the structural analysis of GAG chains primed by fluorophore-tagged xyloside **9** could not be studied using fluorescent detectors and relied instead on radiometric detector.

The UMB-*O*-xyloside has been shown to function as acceptor for the elongation of GAG chains by several groups. However, this well-known fluorophore-tagged xyloside mostly prime CS with low MW chains.[15,17] By changing the *O* linkage of the fluorophore-tagged xyloside to click linkage, the fluorophore-tagged click-xylosides were predicted to prime both HS and CS with higher MW chains as many other click-xylosides. The results from priming activity analysis suggest that optimized priming concentration of UMB-click-xylosides **13a** and **13b** is 300 μM. Therefore, the GAG chains primed in CHO cells by these xylosides at 300 μM were further analyzed for their molecular weight using the size exclusion column and HS/CS composition using heparitinase I, II, and III. It is interesting to note that both fluorophore-tagged click-xylosides **13a** and **13b** primed GAG chains whose average molecular weight (42 kDa) is higher than those primed by commercial UMB-*O*-xyloside (4 kDa) (Figure 2). Furthermore, it is surprising to note that fluorophore-tagged click-xylosides **13a** and **13b** primed about 30% HS chains, whereas commercial UMB-*O*-xylosides primed less than 5% HS chains (Figure 3). Some minor peaks appeared beyond Vt in the size exclusion column, and appearance of these late peaks may be attributed to the interactions of unknown small molecules carrying hydrophobic fluorophore with the column.
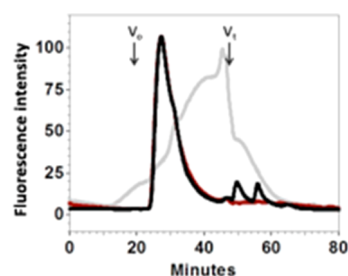

Figure 2. Size exclusion profiles of GAG chains primed by fluorophore-tagged xylosides (UMB-*O*-xyloside, **13a**, and **13b**) in *pgsA*-745 cells. GAG chains primed by fluorophore-tagged xylosides at 300 μM concentration in *pgsA*-745 cells for 24 h. The primed GAG chains were then purified and analyzed as described in the Experimental Section. The elution profile of the GAG chains primed by UMB-*O*-xyloside (gray trace), by fluorophore-tagged xyloside **13a** (red trace), and by fluorophore-tagged xyloside **13b** (black trace).
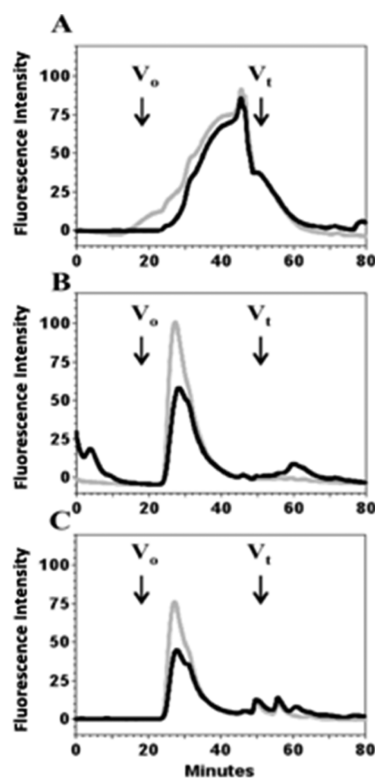

Figure 3. HS/CS compositions of GAG chains primed by fluorophore-tagged xylosides (UMB-*O*-xyloside, **13a**, and **13b**) in *pgsA*-745 cells. GAG chains primed by fluorophore-tagged xylosides at 300 μM concentration in *pgsA*-745 cells for 24 h. The HS/CS composition of the primed GAG chains was determined by digesting the GAG chains with heparitinase I, II, III. The purified GAG chains were analyzed by size exclusion chromatography. The elution profiles of the primed GAG chains without heparitinase I, II, III (gray trace). The elution profiles of the primed GAG chains with heparitinase I, II, III (black trace). (A) The elution profiles of GAG chains primed by UMB-*O*-xyloside. (B) The elution profile of GAG chains primed by fluorophore-tagged click-xyloside **13a**. (C) The elution profiles of GAG chains primed by fluorophore-tagged click-xyloside **13b**.

Structural Analysis of Primed GAG Chains in Endothelial Cells (BLMVEC). The fluorophore-tagged xylosides did prime GAG chains well in endothelial cells at various concentrations. At the optimal concentration (300 μM), molecular weight of GAG chains primed by fluorophore-tagged
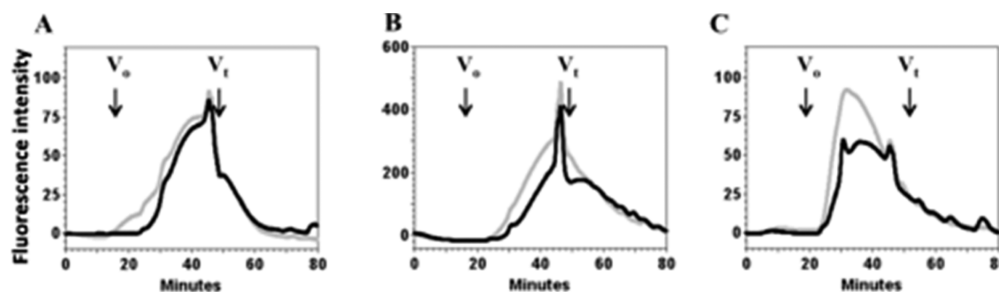
Figure 4. HS/CS compositions of GAG chains primed by fluorophore-tagged xylosides (UMB-*O*-xyloside, **13a**, and **13b**) in endothelial cells. GAG chains primed by fluorophore-tagged xylosides at 300 μM concentration in BLMVEC cells for 24 h. The HS/CS composition of the primed GAG chains was determined by digesting the GAG chains with heparitinase I, II, and III. The purified GAG chains were analyzed by size exclusion chromatography. The elution profiles of the primed GAG chains before heparitinase I, II, III treatment (gray trace). The elution profiles of the primed GAG chains after heparitinase I, II, III (black trace). (A) The elution profiles of GAG chains primed by UMB-*O*-xyloside. (B) The elution profile of GAG chains primed by fluorophore-tagged click-xyloside **13a**. (C) The elution profile of GAG chains primed by fluorophore-tagged click-xyloside **13b**.

xyloside **13b** is much higher than those primed by commercial UMB-*O*-xyloside but the molecular weight of GAG chains primed by fluorophore-tagged xyloside **13a** is not higher than those primed by commercial UMB-*O*-xyloside. The highly electron withdrawing substituent of $-CF_3$ may result in longer GAG chains in BLMVEC cells. These GAG chains primed by fluorophore-tagged xylosides **13a** and **13b** and commercial UMB-*O*-xyloside were digested with heparitinase I/II/III to determine the percentage of HS. These fluorophore-tagged click-xylosides produced a significant amount of HS than the commercial xyloside as shown in Figure 4.

CONCLUSIONS

A small library of novel fluorophore-tagged xylosides was synthesized to evaluate their GAG-priming activity. Pyrene-click-xyloside **9** and UMB-click-xylosides **13a** and **13b** were able to participate in the stimulation of GAG biosynthesis. These fluorophore-tagged xylosides containing the triazyol rings were more stable than commercially available xylosides and predictably have a longer in vivo half-life. Moreover, they were able to prime a significant amount of HS chains and higher MW than a commercial fluorophore-tagged *O*-xyloside. Therefore, these novel fluorophore-tagged click-xylosides have the potential to profile and elucidate cellular-specific GAG chains to define various dynamic interactions in the complex systems and to offer prospects to further our understanding of factors that regulate GAG biosynthesis as well as new knowledge on the role of GAG chains in various signaling events associated with pathophysiological processes.

ASSOCIATED CONTENT

Ⓢ Supporting Information

Experimental data and NMR spectra. This material is available free of charge via the Internet at http://pubs.acs.org.

AUTHOR INFORMATION

Corresponding Author

*Tel. 801-587-9474; Fax. 801-585-9119; E-mail: KUBY@ pharm.utah.edu.

Notes

The authors declare no competing financial interest.

ACKNOWLEDGMENTS

REFERENCES

(1) Kramer, K. L. (2010) Specific sides to multifaceted glycosaminoglycans are observed in embryonic development. *Semin. Cell. Dev. Biol. 21*, 631−7.

(2) Perrimon, N., and Bernfield, M. (2000) Specificities of heparan sulphate proteoglycans in developmental processes. *Nature 404*, 725−8.

(3) Iozzo, R. V. (2005) Basement membrane proteoglycans: from cellar to ceiling. *Nat. Rev. Mol. Cell. Biol. 6*, 646−56.

(4) Ringvall, M., and Kjellen, L. (2010) Mice deficient in heparan sulfate *N*-deacetylase/*N*-sulfotransferase 1. *Prog. Mol. Biol. Transl. Sci. 93*, 35−58.

(5) Sasisekharan, R., Shriver, Z., Venkataraman, G., and Narayanasami, U. (2002) Roles of heparan-sulphate glycosaminoglycans in cancer. *Nat. Rev. Cancer 2*, 521−8.

(6) Bernfield, M., Gotte, M., Park, P. W., Reizes, O., Fitzgerald, M. L., Lincecum, J., and Zako, M. (1999) Functions of cell surface heparan sulfate proteoglycans. *Annu. Rev. Biochem. 68*, 729−77.

(7) Sasisekharan, R., Raman, R., and Prabhakar, V. (2006) Glycomics approach to structure-function relationships of glycosaminoglycans. *Annu. Rev. Biomed. Eng. 8*, 181−231.

(8) Vassal-Stermann, E., Duranton, A., Black, A. F., Azadiguian, G., Demaude, J., Lortat-Jacob, H., Breton, L., and Vives, R. R. (2012) A new C-xyloside induces modifications of GAG expression, structure and functional properties. *PLoS One 7*, e47933.

(9) Kuberan, B., Ethirajan, M., Victor, X. V., Tran, V., Nguyen, K., and Do, A. (2008) "Click" xylosides initiate glycosaminoglycan biosynthesis in a mammalian cell line. *ChemBioChem 9*, 198−200.

(10) Victor, X. V., Nguyen, T. K., Ethirajan, M., Tran, V. M., Nguyen, K. V., and Kuberan, B. (2009) Investigating the elusive mechanism of glycosaminoglycan biosynthesis. *J. Biol. Chem. 284*, 25842−53.

(11) Fukunaga, Y., Sobue, M., Suzuki, N., Kushida, H., and Suzuki, S. (1975) Synthesis of a fluorogenic mucopolysaccharide by chondrocytes in cell culture with 4-methylumbelliferyl beta-D-xyloside. *Biochim. Biophys. Acta 381*, 443−7.

(12) Lugemwa, F. N., and Esko, J. D. (1991) Estradiol beta-D-xyloside, an efficient primer for heparan sulfate biosynthesis. *J. Biol. Chem. 266*, 6674−7.

(13) Fritz, T. A., Lugemwa, F. N., Sarkar, A. K., and Esko, J. D. (1994) Biosynthesis of heparan sulfate on beta-D-xylosides depends on aglycone structure. *J. Biol. Chem. 269*, 300−7.

(14) Malmberg, J., Mani, K., Sawen, E., Wiren, A., and Ellervik, U. (2006) Synthesis of aromatic *C*-xylosides by position inversion of glucose. *Bioorg. Med. Chem. 14*, 6659−65.

(15) Salimath, P. V., Spiro, R. C., and Freeze, H. H. (1995) Identification of a novel glycosaminoglycan core-like molecule. II. Alpha-GalNAc-capped xylosides can be made by many cell types. *J. Biol. Chem. 270*, 9164−8.

(16) Freeze, H. H., Sampath, D., and Varki, A. (1993) Alpha- and beta-xylosides alter glycolipid synthesis in human melanoma and Chinese hamster ovary cells. *J. Biol. Chem. 268*, 1618−27.

(17) Shibata, S., Takagaki, K., Ishido, K., Konn, M., Sasaki, M., and Endo, M. (2003) HNK-1-Reactive oligosaccharide, sulfate-*O*-3GlcA-beta1−4Xylbeta1-MU, synthesized by cultured human colorectal cancer cells. *Tohoku. J. Exp. Med. 199*, 13−23.

(18) (a) Johnsson, R., Mani, K., and Ellervik, U. (2007) Evaluation of fluorescently labeled xylopyranosides as probes for proteoglycan biosynthesis. *Bioorg. Med. Chem. Lett. 17*, 2338−41. (b) Johnsson, R., Mani, K., Cheng, F., and Ellervik, U. (2006) Regioselective reductive openings of acetals; mechanistic details and synthesis of fluorescently labeled compounds. *J. Org. Chem. 71*, 3444−51.

(19) Sobue, M., Habuchi, H., Ito, K., Yonekura, H., Oguri, K., Sakurai, K., Kamohara, S., Ueno, Y., Noyori, R., and Suzuki, S. (1987) Beta-D-xylosides and their analogues as artificial initiators of glycosaminoglycan chain synthesis. Aglycone-related variation in their effectiveness in vitro and in ovo. *Biochem. J. 241*, 591−601.

(20) Aich, U., and Loganathan, D. (2005) Synthesis of *N*-(Beta-glycopyrano-syl)azidoacetamides. *J. Carbohydr. Chem. 24*, 1−12.

(21) Kolb, H., Finn, M., and Sharpless, K. (2001) Click chemistry: Diverse chemical function from a few good reactions. *Angew. Chem., Int. Ed. 40*, 2004.

(22) Esko, J. D., Stewart, T. E., and Taylor, W. H. (1985) Animal cell mutants defective in glycosaminoglycan biosynthesis. *Proc. Natl. Acad. Sci. U.S.A. 82*, 3197−201.